

AD-A202 841

Electron Paramagnetic Resonance and Photoluminescence Studies of Impurities in CdTe

R. C. BOWMAN, JR.
Chemistry and Physics Laboratory
Laboratory Operations
The Aerospace Corporation
El Segundo, CA 90245-4691

D. E. COOPER
Rockwell International Science Center
Thousand Oaks, CA 91360

31 October 1988

Prepared for
SPACE DIVISION
AIR FORCE SYSTEMS COMMAND
Los Angeles Air Force Base
P.O. Box 92960, Worldway Postal Center
Los Angeles, CA 90009-2960

DTIC
ELECTE
S **D**
DEC 19 1988
8E

APPROVED FOR PUBLIC RELEASE;
DISTRIBUTION UNLIMITED

DEC 12 1988

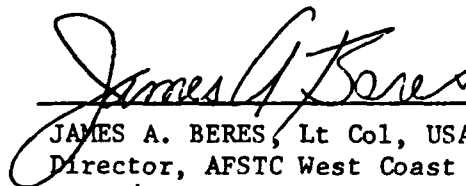
This report was submitted by The Aerospace Corporation, El Segundo, CA 90245, under Contract No. F04701-85-C-0086-P00016 with the Space Division, P.O. Box 92960, Worldway Postal Center, Los Angeles, CA 90009-2960. It was reviewed and approved for The Aerospace Corporation by S. Feuerstein, Director, Chemistry and Physics Laboratory. Capt Brad Biehn, SD/CNSS, was the project officer for the Mission-Oriented Investigation and Experimentation (MOIE) Program.

This report has been reviewed by the Public Affairs Office (PAS) and is releasable to the National Technical Information Service (NTIS). At NTIS, it will be available to the general public, including foreign nationals.

This technical report has been reviewed and is approved for publication. Publication of this report does not constitute Air Force approval of the report's findings or conclusions. It is published only for the exchange and stimulation of ideas.



BRADLEY BIEHN, Capt, USAF
MOIE Project Officer
SD/CNSS



JAMES A. BERES, Lt Col, USAF
Director, AFSTC West Coast Office
AFSTC/WCO

UNCLASSIFIED

SECURITY CLASSIFICATION OF THIS PAGE

ADA202841

REPORT DOCUMENTATION PAGE

1a. REPORT SECURITY CLASSIFICATION Unclassified			1b. RESTRICTIVE MARKINGS			
2a. SECURITY CLASSIFICATION AUTHORITY			3. DISTRIBUTION / AVAILABILITY OF REPORT Approved for public release; distribution unlimited.			
2b. DECLASSIFICATION / DOWNGRADING SCHEDULE			5. MONITORING ORGANIZATION REPORT NUMBER(S) SD-TR-88-100			
4. PERFORMING ORGANIZATION REPORT NUMBER(S) TR-0088(3945-07)-4			7a. NAME OF MONITORING ORGANIZATION Space Division			
6a. NAME OF PERFORMING ORGANIZATION The Aerospace Corporation Laboratory Operations		6b. OFFICE SYMBOL (if applicable)		7b. ADDRESS (City, State, and ZIP Code) Los Angeles Air Force Base Los Angeles, CA 90009-2960		
6c. ADDRESS (City, State, and ZIP Code) El Segundo, CA 90245			9. PROCUREMENT INSTRUMENT IDENTIFICATION NUMBER F04701-85-C-0086-P00019			
8a. NAME OF FUNDING / SPONSORING ORGANIZATION		8b. OFFICE SYMBOL (if applicable)		10. SOURCE OF FUNDING NUMBERS		
8c. ADDRESS (City, State, and ZIP Code)			PROGRAM ELEMENT NO.	PROJECT NO.	TASK NO.	WORK UNIT ACCESSION NO.
11. TITLE (Include Security Classification) Electron Paramagnetic Resonance and Photoluminescence Studies of Impurities in CdTe						
12. PERSONAL AUTHOR(S) Bowman, R. C., Jr.; Cooper, D. E. (Rockwell Int. Science Center)						
13a. TYPE OF REPORT		13b. TIME COVERED FROM TO		14. DATE OF REPORT (Year, Month, Day) 31 October 1988		15. PAGE COUNT 11
16. SUPPLEMENTARY NOTATION						
17. COSATI CODES			18. SUBJECT TERMS (Continue on reverse if necessary and identify by block number)			
FIELD	GROUP	SUB-GROUP	Electron paramagnetic resonance, Impurities in compound semiconductors, <i>Iron, Cadmium Telluride</i> Defects in compound semiconductors, <i>(Align)</i>			
19. ABSTRACT (Continue on reverse if necessary and identify by block number)						
<p>✓ CdTe single crystals from different sources have been examined to detect the presence of impurities which may be detrimental to applications in the fabrication of infrared detectors. Distinctive EPR signals from various donor impurities, including substitutional paramagnetic Fe, were found in several samples. A photoluminescence transition at 1.1 eV was also seen in these crystals and the amplitudes of the photoluminescence signals and the Fe EPR signals are strongly correlated. Elemental analysis of the samples indicates that EPR and PL are able to detect Fe concentrations of less than 0.1 ppm.</p>						
20. DISTRIBUTION / AVAILABILITY OF ABSTRACT <input type="checkbox"/> UNCLASSIFIED/UNLIMITED <input checked="" type="checkbox"/> SAME AS RPT. <input type="checkbox"/> DTIC USERS				21. ABSTRACT SECURITY CLASSIFICATION Unclassified		
22a. NAME OF RESPONSIBLE INDIVIDUAL			22b. TELEPHONE (Include Area Code)		22c. OFFICE SYMBOL	

DD FORM 1473, 84 MAR

83 APR edition may be used until exhausted.
All other editions are obsolete.

SECURITY CLASSIFICATION OF THIS PAGE

UNCLASSIFIED

UNCLASSIFIED

SECURITY CLASSIFICATION OF THIS PAGE

18. SUBJECT TERMS (Continued)

Photoluminescence in II-VI semiconductors

UNCLASSIFIED

SECURITY CLASSIFICATION OF THIS PAGE

PREFACE

We wish to thank S. Witt and P. Smith of Caltech for assistance with the EPR measurements, R. Robertson for preparing many of the samples, and J. Bajaj for several fruitful discussions. M. Locke performed the ICP/AE analysis, and L. Bubulac assisted with the SIMS analysis.

Accession For	
NEIS CRA&I	<input checked="" type="checkbox"/>
DEIC TAB	<input checked="" type="checkbox"/>
Unannounced	<input type="checkbox"/>
Justification	
By _____	
Distribution/	
Availability Codes	
Dist	Avail and/or Special
A-1	



Many factors can influence the performance of infrared detectors fabricated from $\text{Hg}_{1-x}\text{Cd}_x\text{Te}$. One important factor is impurities from the substrate (typically CdTe or a related alloy) that is used during the epitaxial growth of a $\text{Hg}_{1-x}\text{Cd}_x\text{Te}$ film. For example, Fe impurities reduce the minority carrier lifetime of $\text{Hg}_{1-x}\text{Cd}_x\text{Te}$ (Ref. 1), which will impair detector performance. Although considerable improvements in the chemical purity and structural quality of these CdTe crystals have been made in recent years, it can be very difficult to identify and measure the contamination level of potentially harmful impurities that occur at concentrations in the parts-per-million range. Nondestructive techniques such as electron paramagnetic resonance (EPR) and photoluminescence (PL) can be very useful for screening materials used in fabricating infrared detectors. We have applied these techniques to several nominally pure CdTe single-crystal wafers intended for use as substrates for the liquid-phase epitaxy of $\text{Hg}_{1-x}\text{Cd}_x\text{Te}$. Past EPR studies on CdTe have identified various impurities such as transition metals (Refs. 2-4), shallow donor (Refs. 5,6) and deep donor (Refs. 7,8). Numerous PL studies have been carried out to characterize the impurities and defects in CdTe samples (Refs. 6,9-13), and in several cases impurities can be identified by unique PL lines. Recently, Lischka et al. (Ref. 10) observed PL peaks at 1.475 eV (i.e., 840 nm) and 1.1 eV (1130 nm) in Fe-implanted CdTe that they attributed to iron impurities. However, this group has since recanted the assignment of the 1.475 eV peak to an iron-related center, while still assigning the 1.1 eV peak to Fe impurities (Ref. 12). Our results with undoped samples show a strong correlation between the distinctive EPR signal from Fe^{+3} and the amplitude of the 1.1 eV PL line, which supports this assignment. The 1.475 eV peak has been observed by other workers in the PL spectra of epitaxial CdTe, and is probably due to a crystalline defect (Refs. 14-16). In our PL experiments on CdTe there was no correlation of the 1.475 eV peak with the presence of iron as seen by EPR measurements. Thus our results confirm the assignment of the 1.1 eV PL line as due to deep levels associated with Fe impurities, and indicate that Fe is a significant impurity in CdTe with large sample-to-sample variations in concentration.

CdTe wafers with both (111) and (100) faces were obtained from a number of commercial sources. The EPR experiments were performed in the x-band frequency range at temperatures between 5K and 20K, and no significant temperature effects were observed. Photo-excited EPR measurements were obtained in-situ with focused light from an unfiltered 200-watt Hg-Xe lamp. For PL spectroscopy, the samples were etched in bromine-methanol solutions to obtain high-quality surfaces, and cooled to 15K in a closed-cycle helium refrigerator. They were excited by an Ar⁺ laser at 514.5 nm, and the resulting PL was dispersed by a monochromator and detected with a cooled germanium detector.

A portion of the EPR spectrum obtained from CdTe crystal No. 2438-1 at 6.5K is presented in Fig. 1. A large number of peaks are seen, and their intensities and positions are extremely dependent upon the orientation of the crystal with respect to the magnetic field. However, most of these transitions were found to correspond to the highly anisotropic spectrum (Ref. 4) for the isolated Fe⁺³ ion when it occupies Cd sites in the CdTe lattice. The only other distinguishable paramagnetic species present in this crystal is the relatively weak octet near 2800 gauss that corresponds to the Co⁺² ion (Ref. 2). When this sample was illuminated with the unfiltered lamp, the intensities of the iron peaks decreased by about 25-30%, but no new features were observed.

EPR measurements were made on a CdTe crystal that was deliberately doped with about 2×10^{17} indium atoms/cm³. Since this sample has a resistivity above $10^8 \Omega\text{-cm}$, the indium donor atoms are highly compensated. While no EPR signal was seen without illumination, a single isotropic peak corresponding to a g-factor of 1.694 was found under photoexcitation. This behavior is very similar to that described by Saminadayar (Ref. 5), who reported a peak with g-factor 1.704(1) and peak-to-peak linewidth (ΔH_{pp}) of 22 gauss from their In-doped samples. Figure 2 shows the EPR spectra for three CdTe samples that had not been intentionally doped with any potential donor. Under lamp illumination, all three crystals yield the donor EPR spectral line. In addition, sample Nos. 4-7 had several of the peaks that correspond to the iron (Fe⁺³) impurity.

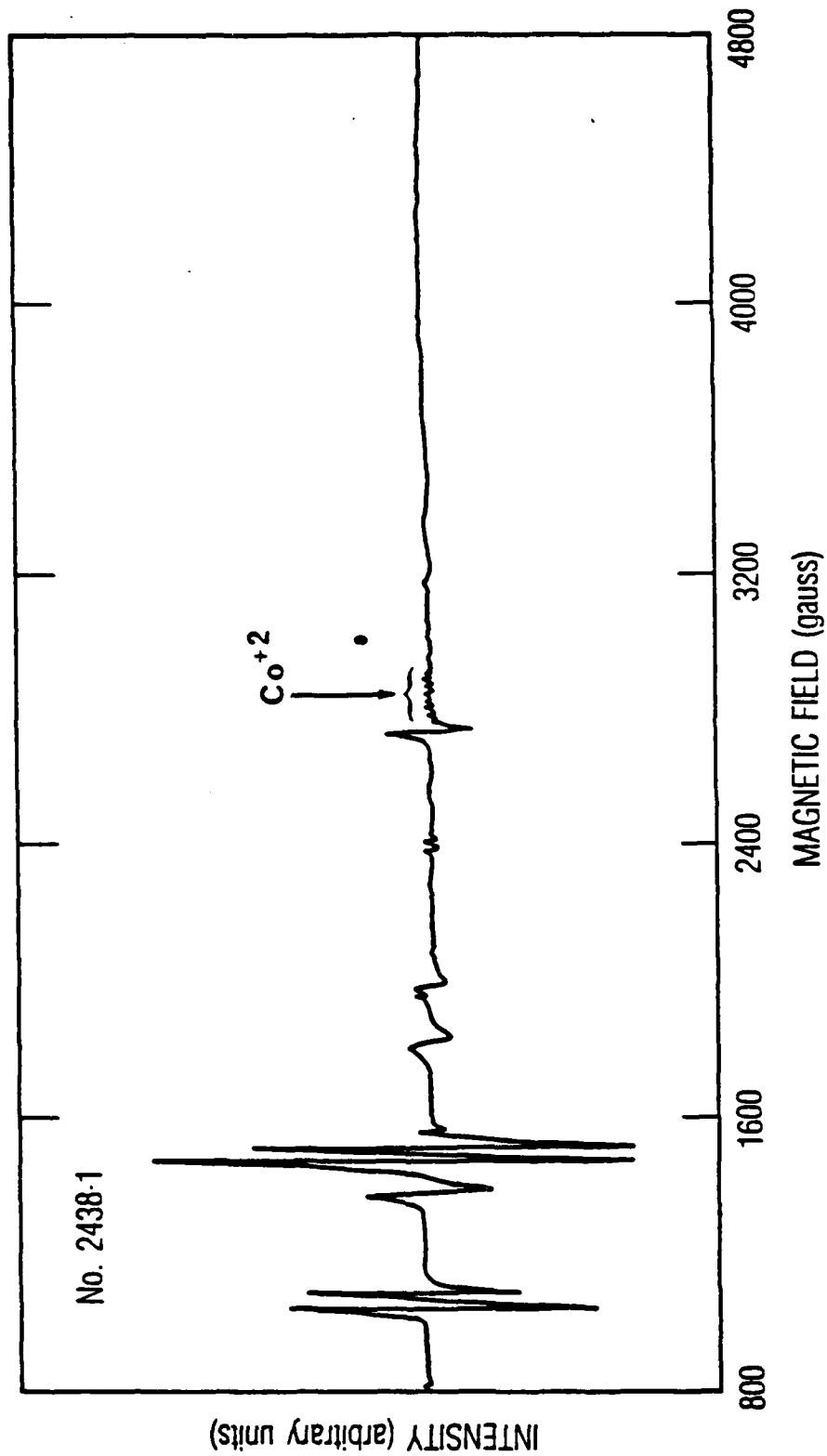


Fig. 1. EPR spectrum for CdTe crystal No. 2438-1 with (111)-axis roughly aligned with magnetic field. Most peaks can be attributed to isolated Fe⁺³ center except for much weaker octet near 2800G from Co⁺² ion.

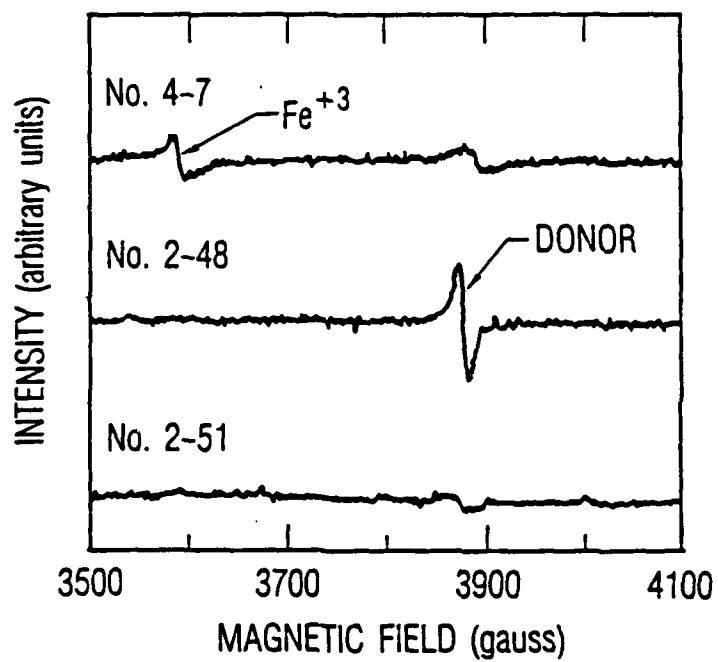


Fig. 2. EPR spectra for three different CdTe crystals while illuminated with unfiltered light

EPR measurements were made on samples from nearly 20 different crystals that had been obtained from various sources and commercial suppliers. Some crystals had also been further processed by multi-zone refining or extended thermal annealing at 600°C under equilibrium Cd vapor pressure. Results for several of these CdTe samples are presented in Table 1. Other than the previously described sample, No. 2438-1, the only paramagnetic centers detected were substitutional Fe⁺³ or the shallow donor center. A few crystals gave no EPR transitions, despite considerable efforts made to detect the centers previously reported (Refs. 2-8) for CdTe. However, it must be remembered that most of these samples were intended to be substrates for Hg_{1-x}Cd_xTe film growth and were prepared from high-purity starting materials. Consequently, the presence of even these impurities was not anticipated.

Table 1. Summary of EPR Measurements on CdTe Crystals at X-Band Frequencies and Temperatures Between 5K and 15K

Sample	Original Source	Fe Signals	Donor		Comments
			G-Factor	ΔHpp(G)	
2438-1	II-VI	Yes	ND	--	Weak Co ⁺²
4011-1	II-VI	ND	1.604	18	2 × 10 ¹⁷ In/cm ³
2303	II-VI	Yes	ND	--	Cu Doped (= 1 ppm)
2-48	NMC	ND	1.699	10	As-Received
4-7	Cominco	Yes	1.693	20	Rockwell Regrown
QZR-217	Cominco	ND	ND	--	Quadruple Zone-Refined
1949	Rockwell	ND	ND	--	As-Grown
1949-A	Rockwell	ND	ND	--	600°C Cd Annealed

ND = Not Detected

The photoluminescence spectra in the region near 1.0 eV are shown in Fig. 3 for four CdTe crystals. The largest PL intensity occurs for sample No. 2438-1, which also gave the strongest Fe⁺³ EPR signal. This PL feature is asymmetric and seems to consist of two partly resolved components at 1.13 eV

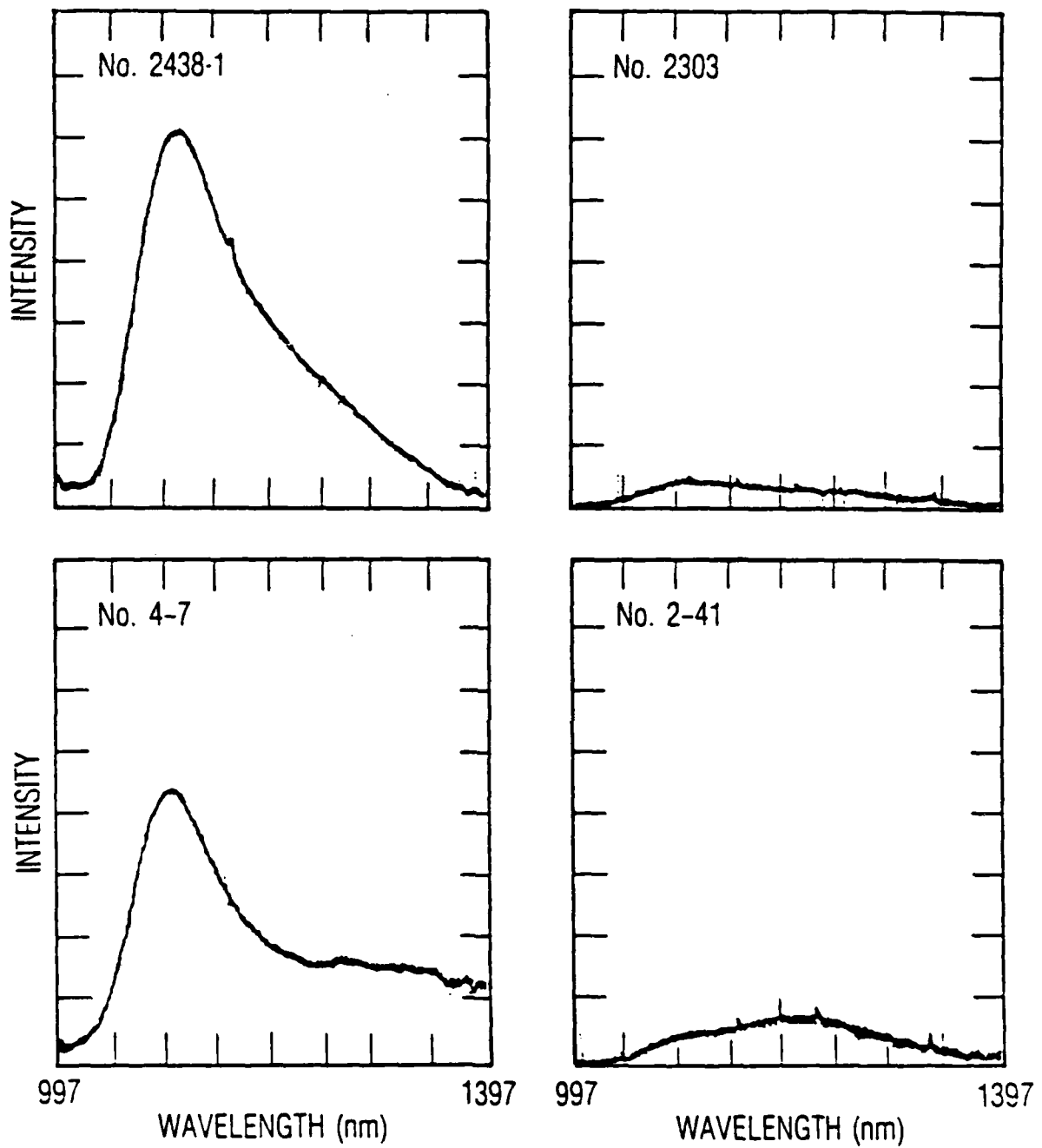


Fig. 3. Low temperature photoluminescence spectra for four CdTe crystals in regions of 1.0 eV peaks

(1.1 μm) and about 1.03 eV (1.2 μm). These transitions were also attributed to Fe transitions in iron-implanted CdTe by Kernocker et al. (Ref. 12). There is considerable variation in the PL intensity and lineshape among the samples.

In Table 2 we directly compare the intensities of the strongest Fe^{+3} EPR peak with the amplitude of the 1.13 eV PL component for several CdTe samples. A general consistency is found in that the crystal with the largest Fe^{+3} EPR signal also has the most intense PL peak, whereas samples without the iron EPR signal had the smallest PL intensities. However, a quantitative linear correlation was not seen. Several factors can be responsible. First, only the Fe^{+3} ions with $3d^5$ electrons in the $S = 5/2$ state are readily detected by EPR (i.e., the Fe^{+2} and Fe^+ ions are not usually seen). The charge state of the iron atom in the crystal depends on the ionization energy of the ion relative to the Fermi level. Thus, in an n-type sample the iron will tend to be in the form of Fe^{+2} and will not be detected by EPR. Iron in the +2 state can be converted to the +3 state by absorption of near-IR photons, but illuminations with unfiltered and selectively filtered light did not produce any enhancements in the Fe^{+3} EPR signals such as had been seen in some CdTe crystals by Lischka et al. (Ref. 10). Hence, we believe the EPR measurements are providing good estimates of the relative amounts of iron present in each CdTe crystal, even though the absolute contents cannot be determined by this method. One further difficulty with the Fe^{+3} EPR signals is the multiline nature of its spectrum (Ref. 4), which is also extremely dependent upon crystal orientation. This feature limits any quantitative measure of the total intensity of the Fe^{+3} spectrum. On the other hand, the PL experiments are also not very quantitative due to variations in the radiative efficiency of the PL emission. For example, crystal No. 2303 had been intentionally grown with a nominal 1 ppm of copper which may have caused a quenching of the PL emission. To check this hypothesis, we compared the PL intensity at 1.13 eV with that near the band edge at 1.6 eV. The near-band-edge peak for No. 2303 is more than four times smaller than that of No. 2438-1, suggesting that substantial quenching is occurring due to the copper doping.

Table 2. Normalized Intensities of Fe⁺³ EPR Signal and PL Peak at 1.13 eV Compared with Total Fe Concentration from ICP/AE

Sample	EPR	PL	Fe Concentration (ppm)
2438-1	1.0	1.0	< 0.67
100	0.28	0.64	--
4-7	0.20	0.50	< 0.6
CP2-A	0.39	0.40	1 ± 0.8
2-42	0.0	0.09	< 0.55
2-48	0.0	0.09	< 0.85
2-41	0.0	0.08	< 0.55
2303	0.05	0.06	< 0.38
1949	0.0	0.05	< 0.91
QZR-217	0.0	0.02	1.2 ± 0.65

Although the amplitude of the 1.13 eV peak correlates well with the amplitude of the EPR signal for Fe⁺³, the low-energy shoulder of this peak, which includes a poorly-resolved component at about 1.03 eV, presents a more complex picture. Two samples with large 1.13 eV peaks (No. 2438-1 and No. 100) had PL spectra with substantial shoulders in the 1.03 eV region. However, the spectra of two of the samples containing Fe (No. 4-7 and No. CP2-A) had continued PL emission down to (and presumably beyond) 0.9 eV, and although there was considerable PL intensity at 1.03 eV, no shoulder could be discerned. Two of the samples with no Fe⁺³ EPR signal (No. 2-41 and No. 2-42) had more PL emission in the lower energy region than at 1.13 eV, and all samples showed weak emission at both 1.13 and 1.03 eV. This suggests that although Fe probably contributes to PL emission at 1.03 eV, other defects and impurities also cause PL in the 0.9-1.1 eV region. Since the residual emission from these unidentified sources appears to be lower at 1.13 than 1.03 eV, the PL emission at 1.13 eV is a better indicator of the Fe content of a CdTe sample.

Table 2 also lists the concentration of Fe in the samples as measured by inductively coupled plasma/atomic emission spectrometry (ICP/AE). Little or no correlation is seen between these data and the EPR and PL results. This could possibly result from the fact that ICP/AE measure the total Fe content, while EPR (and possibly PL) is only sensitive to the Fe^{+3} concentration. Thus, most of the iron content seen by ICP/AE could be in the +2 state or dissolved in tellurium inclusions (Ref. 17). Two of the samples, No. 100 and No. 2-41, were also analyzed by SIMS, which requires less material than ICP/AE and is more sensitive. Both samples showed an iron signal corresponding to a content of about 0.1 ppm. In view of the large difference in the iron PL and EPR signals from these samples, this level probably corresponds to the background interference from Cd^{+2} ions. Thus the threshold for PL detection of iron in CdTe is better than 0.1 ppm, which is exceeded only by destructive techniques using large (> 1 gm) samples.

The initial results of using EPR and PL to detect and quantify specific impurities (e.g., iron and generic shallow donors) are quite encouraging. A good correlation between the Fe^{+3} EPR signal and a PL peak near 1.13 eV has been demonstrated, and the sensitivity of these techniques is excellent. These results appear to verify the recent conclusions of Kernkocker et al. (Ref. 12) that these spectra both arise from iron and can be used to monitor the Fe impurity content in CdTe. In addition, this study makes use of the random variation in Fe concentration in a variety of CdTe samples rather than using Fe implantation to create samples with a large Fe impurity concentration, thus avoiding potential defect formation due to lattice damage during implantation. The PL emission at 1.03 eV is also enhanced by Fe impurities, although other impurities and defects contribute to emission in this region. Future work should include PL and EPR measurements on CdTe samples with Fe impurity levels that can be detected by quantitative analytical methods in order to establish the absolute sensitivity of these techniques. The use of EPR and PL as sensitive, nondestructive diagnostics for Fe impurities will facilitate studies to correlate the Fe concentration of CdTe substrates with the characteristics of HgCdTe layers subsequently grown on the CdTe.

REFERENCES

1. P. Capper, J. Crystal Growth **57**, 280 (1982).
2. R. S. Title, in Physics and Chemistry of II-VI Compounds, edited by M. Aven and J. S. Prener (American Elsevier, New York, 1967) p. 265.
3. U. Kaufman, J. Windschief, and G. Brunthaler, J. Phys. C: Solid State Phys. **17**, 6169 (1984).
4. G. Brunthaler, U. Kaufmann, and J. Schneider, J. Appl. Phys. **56**, 2974 (1984).
5. K. Saminadayar, D. Galland, and E. Molva, Solid State Commun. **49**, 627 (1984).
6. K. Saminadayar, J. M. Francou, and J. L. Poutrat, J. Cryst. Growth **72**, 236 (1985).
7. R. C. duVarney and A. K. Garrison, Phys. Rev. B **12**, 10 (1975).
8. G. Brunthaler, W. Jantsch, U. Kaufmann, and J. Schneider, Phys. Rev. B **31**, 1239 (1985).
9. K. Zanio, in Cadmium Telluride - Semiconductors and Semimetals, Vol. 13, edited by R. K. Willardson and A. C. Beer (Academic, New York, 1978).
10. K. Lischka, G. Brunthaler, and W. Jantsch, J. Cryst. Growth **72**, 335 (1985).
11. J. L. Pautrat, J. M. Francou, N. Magnea, E. Molva, and K. Saminadayar, J. Cryst. Growth **72**, 194 (1985).
12. R. Kernocker, K. Lischka, and L. Palmetshofer, J. Cryst. Growth **86**, 625 (1988).
13. D. E. Cooper, J. Bajaj, and P. R. Newman, J. Cryst. Growth **86**, 544 (1988).
14. P. J. Dean, G. M. Williams, and G. Blackmore, J. Phys. D **17**, 2291 (1984).
15. Z. C. Feng, A. Muscarenas, and W. J. Choyke, J. Lumin. **35**, 329 (1986).
16. D. J. Lepold, J. M. Ballingall, and M. L. Wroge, Appl. Phys. Lett. **49**, 1473 (1986).
17. J. L. Pantrat, J. M. Francou, N. Magnea, E. Molva, and K. Saminadayar, J. Cryst. Growth **72**, 194 (1985).

LABORATORY OPERATIONS

The Aerospace Corporation functions as an "architect-engineer" for national security projects, specializing in advanced military space systems. Providing research support, the corporation's Laboratory Operations conducts experimental and theoretical investigations that focus on the application of scientific and technical advances to such systems. Vital to the success of these investigations is the technical staff's wide-ranging expertise and its ability to stay current with new developments. This expertise is enhanced by a research program aimed at dealing with the many problems associated with rapidly evolving space systems. Contributing their capabilities to the research effort are these individual laboratories:

Aerophysics Laboratory: Launch vehicle and reentry fluid mechanics, heat transfer and flight dynamics; chemical and electric propulsion, propellant chemistry, chemical dynamics, environmental chemistry, trace detection; spacecraft structural mechanics, contamination, thermal and structural control; high temperature thermomechanics, gas kinetics and radiation; cw and pulsed chemical and excimer laser development including chemical kinetics, spectroscopy, optical resonators, beam control, atmospheric propagation, laser effects and countermeasures.

Chemistry and Physics Laboratory: Atmospheric chemical reactions, atmospheric optics, light scattering, state-specific chemical reactions and radiative signatures of missile plumes, sensor out-of-field-of-view rejection, applied laser spectroscopy, laser chemistry, laser optoelectronics, solar cell physics, battery electrochemistry, space vacuum and radiation effects on materials, lubrication and surface phenomena, thermionic emission, photosensitive materials and detectors, atomic frequency standards, and environmental chemistry.

Computer Science Laboratory: Program verification, program translation, performance-sensitive system design, distributed architectures for spaceborne computers, fault-tolerant computer systems, artificial intelligence, microelectronics applications, communication protocols, and computer security.

Electronics Research Laboratory: Microelectronics, solid-state device physics, compound semiconductors, radiation hardening; electro-optics, quantum electronics, solid-state lasers, optical propagation and communications; microwave semiconductor devices, microwave/millimeter wave measurements, diagnostics and radiometry, microwave/millimeter wave thermionic devices; atomic time and frequency standards; antennas, rf systems, electromagnetic propagation phenomena, space communication systems.

Materials Sciences Laboratory: Development of new materials: metals, alloys, ceramics, polymers and their composites, and new forms of carbon; non-destructive evaluation, component failure analysis and reliability; fracture mechanics and stress corrosion; analysis and evaluation of materials at cryogenic and elevated temperatures as well as in space and enemy-induced environments.

Space Sciences Laboratory: Magnetospheric, auroral and cosmic ray physics, wave-particle interactions, magnetospheric plasma waves; atmospheric and ionospheric physics, density and composition of the upper atmosphere, remote sensing using atmospheric radiation; solar physics, infrared astronomy, infrared signature analysis; effects of solar activity, magnetic storms and nuclear explosions on the earth's atmosphere, ionosphere and magnetosphere; effects of electromagnetic and particulate radiations on space systems; space instrumentation.